Ordering of Poly(3-hexylthiophene) Nanocrystallites on the Basis of Substrate Surface Energy

Bryce Meredig,[†] Alberto Salleo,[‡] and Richard Gee[†,*]

[†]Lawrence Livermore National Laboratory, Livermore, California 94551, and [‡]Department of Materials Science and Engineering, Stanford University, Stanford, California 94305

ABSTRACT Molecular dynamics simulations are used to study the influence of functionalized substrates on the orientation of poly(3-hexylthiophene) (P3HT) nanocrystallites, which in turn plays a critical role in P3HT-based transistor performance. The effects of alkyl-trichlorosilane self-assembled monolayer packing density, packing order, and end-group functionality are independently investigated. Across these factors, the potential energy surface presented by the substrate to the P3HT molecules is determined to be the main driver of P3HT ordering. Surprisingly, disordered substrates with a smoothly varying potential energy landscape are found to encourage edge-on P3HT orientation, while highly ordered substrates have undesirable potential energy wells that reduce the edge-on orientation of P3HT because of substrate−side-chain interactions.

KEYWORDS: OTFT · P3HT · morphology · ordering · molecular dynamics · OTS · substrate

Organic electronic devices are being actively investigated for application areas where the use of conventional Si-based devices is impractical, too expensive, or impossible, such as solution-coated large-area solar cells and inkjet-printable electronic circuits. One of the most studied semiconductors for organic thin-film transistors (OTFTs) is poly-3-hexylthiophene (P3HT). P3HT is solution-processable, exhibits a relatively high charge carrier mobility (>0.1 $cm^2/(V \cdot s)$)[1] and is commercially available. When cast from solvents into thin films, P3HT has a semicrystalline microstructure composed of nanoscale (10−50 nm) crystallites and amorphous regions. The performance of P3HT OTFTs is strongly affected by the microstructure of the semiconductor layer,[2−11] while the lack of control over this microstructure has severely hampered further progress in the development of improved P3HT-based applications (e.g., solar cells, thin film electronics, *etc.*).[12,13]

A key factor in determining the microstructure of P3HT is the nature of the substrate/semiconductor interface. Indeed, P3HT crystallites in a cast film nucleate at the substrate surface upon evaporation of the solvent.[14,15] Moreover, in bottom-gate OTFT configurations this interface is of particular significance because it is the location of the charge accumulation layer. Substrate−polymer interactions are known to affect the microstructure of the semicrystalline semiconductor, thereby influencing carrier mobility.[16] The highest charge carrier mobility in the plane of the substrate is observed when both the alkyl chains and the thiophene rings of the P3HT crystallites are normal to the substrate (edge-on orientation).[1,2,4,17] However, the specific substrate characteristics that govern P3HT ordering remain largely unknown and are extremely difficult to investigate experimentally due to the buried nature of the P3HT−substrate interface. Greater understanding of these interactions is fundamentally important to the field of organic electronics, as it will lead to reliably improved device performance. Thus, great interest in illuminating the underlying mechanisms of P3HT ordering persists.[18] In this work we use P3HT as a model polymeric semiconductor to examine, for the first time using computational tools, the problem of engineering P3HT morphology through controlling the interactions between P3HT and the substrate.

Chemically modifying a typical substrate (SiO_2 thermally grown on a Si wafer) with a self-assembled monolayer (SAM) of octadecyl-trichlorosilane (OTS) substantially enhances the device performance of most polymeric semiconductors.[15,19−21] X-ray rocking curves indicate that the angular spread of crystallites about the substrate normal plays an important role in charge transport: the smaller the spread, the better the intergrain electronic coupling.[7,22,23] For instance, treating the dielectric surface with OTS produced a population of P3HT

*Address correspondence to gee10@llnl.gov.

Received for review October 23, 2008 and accepted September 4, 2009.

Published online September 11, 2009.
10.1021/nn800707z CCC: $40.75

TABLE 1. Simulation Names and Results[a]

				ring $\langle S \rangle_{ring}$		side chain $\langle S \rangle$		
trial name	SAM density	SAM order	SAM fluorine fraction	orientational order	value/stdev	orientational order	value/stdev	simulation time (ns)
perfect_layer	1.0	1.0	0.0	low	0.23/0.020	low	0.47/0.013	1.012
dens_75	0.75	1.0	0.0	low*	0.21/0.015	low*	0.49/0.0095	1.097
dens_50	0.5	1.0	0.0	low*	0.12/0.011	low*	0.44/0.010	0.186
bare_substrate	0.0 (no SAM)	N/A	N/A	high	0.75/0.011	high	0.69/0.0095	1.002
order_66	1.0	0.66	0.0	high	0.76/0.022	high	0.70/0.0093	2.999
order_33	1.0	0.33	0.0	low	0.26/0.020	low	0.48/0.013	1.345
order_0	1.0	0.0	0.0	high	0.77/0.032	high	0.70/0.014	1.044
fluor_25	1.0	1.0	0.25	medium	0.45/0.014	medium	0.54/0.012	0.175
fluor_50	1.0	1.0	0.50	medium	0.37/0.018	medium	0.55/0.0098	0.358
fluor_100	1.0	1.0	1.0	medium	0.41/0.013	medium	0.55/0.0097	1.010
control	P3HT only	N/A	N/A	low	0.14/0.010	low	0.45/0.0086	0.423

[a]Density = 1.0 corresponds to 5 OTS molecules nm^{-2}. Order = 1.0 is perfect hexagonal packing. Fluorination = 1.0 is 100% SAM termination with CF_3 groups instead of CH_3. Reported $\langle S \rangle$ values are averages over final 100 ps at intervals of 1 ps (final 20 ps for the shorter runs). Trials with an asterisk (*) next to their $\langle S \rangle$ values exhibited interdigitation among the P3HT side chains and the SAM molecules.

crystallites oriented within an angular spread smaller than 0.03° (limited by the resolution of the rocking curve measurement) up to 1 order of magnitude larger than that produced on hexamethyldisilazane (HMDS)-treated surfaces.[15]

Given that the relative orientation of the polymer crystallites plays such an important role in charge transport, the objective of this work is to study some of the most important substrate properties that affect such orientation. On an ideal OTS-treated substrate, the OTS molecules are nearly fully extended[24] and packed at a high density of roughly 5 chains per nm^2,[25−27] screening the effects of the substrate below. Moreover, when perfectly ordered, the OTS molecules are close-packed on the surface, exhibiting long-range order, in contrast to amorphous silica.[26,28] These facts together indicate that the perfectly packed OTS monolayers used in this study, along with the perturbations we apply, are actually quite realistic. It has also been suggested that the chemical properties of the substrate influence how the P3HT chains pack.[29] Here we independently adjust these physical and chemical properties to determine their effects on desirable edge-on P3HT ordering. Table 1 describes the parameters defining the alkyl-trichlorosilane SAM layer that were varied in the simulations, namely, density, packing order, and end group functionality. A packing order value of 0.33, for example, indicates that 67% of the SAM molecules are randomly displaced from their equilibrium positions in the plane of the substrate by an amount equal to at most half the packing distance in the plane of the substrate.

RESULTS AND DISCUSSION

This study parametrically investigates the significance of substrate monolayer density, packing order, and end-group functionality on P3HT ordering. To this end, we have performed classical molecular dynamics (MD) simulations with a simulation geometry as shown in Figure 1. With periodic boundaries and near-ideal registry between neighboring images, the computations closely represent P3HT crystallites such as those that would be found near the substrate surface in a thin film.

The initial P3HT configuration (Figure 1a) is chosen to be very similar to the nanocrystallites of edge-on oriented low-molecular weight (MW) P3HT observed at the OTS-P3HT interface by Kline *et al.*[15] The key figure of merit considered here is the mean order parameter, $\langle S \rangle$, averaged over all 608 monomers every 1000 timesteps. $\langle S \rangle$ is given by

$$\langle S \rangle = \left(\sum_i \frac{3 \cos^2 \theta_i - 1}{2} \right) / n \qquad (1)$$

where θ is the angle between a monomer vector (defined below) and the substrate normal and n is the total number of side chains. We consider two possibilities for the order parameter: $\langle S \rangle_{sidechain}$, in which case the monomer vector points from the S atom on each thiophene ring to the terminal CH_3 group on the corresponding alkyl chain; and $\langle S \rangle_{ring}$, in which case the monomer vector points from the S atom on each thiophene ring to an opposing C atom on that ring. $\langle S \rangle_{sidechain}$ incorporates side-chain conformational degrees of freedom, while $\langle S \rangle_{ring}$ does not. In both cases, $\langle S \rangle = 1$ corresponds to perfect edge-on orientation and $\langle S \rangle = -0.5$ corresponds to face-on orientation (see Figure 1 inset). All systems studied reach a steady state with respect to $\langle S \rangle$ in under 0.5 ns; however, to confirm that a steady state had indeed been reached, several representative simulations were run for at least 1 ns each. We note from Table 1 that $\langle S \rangle_{sidechain}$ and $\langle S \rangle_{ring}$ correlate perfectly in their trends, and from this point we confine the discussion to $\langle S \rangle_{sidechain}$, or simply $\langle S \rangle$.

We find that our results can be separated in three distinct P3HT side-chain order regimes (see Table 1): (1) $\langle S \rangle$ larger than 0.6 (high orientational order); (2) $\langle S \rangle$ between 0.6 and 0.5 (intermediate orientational order);

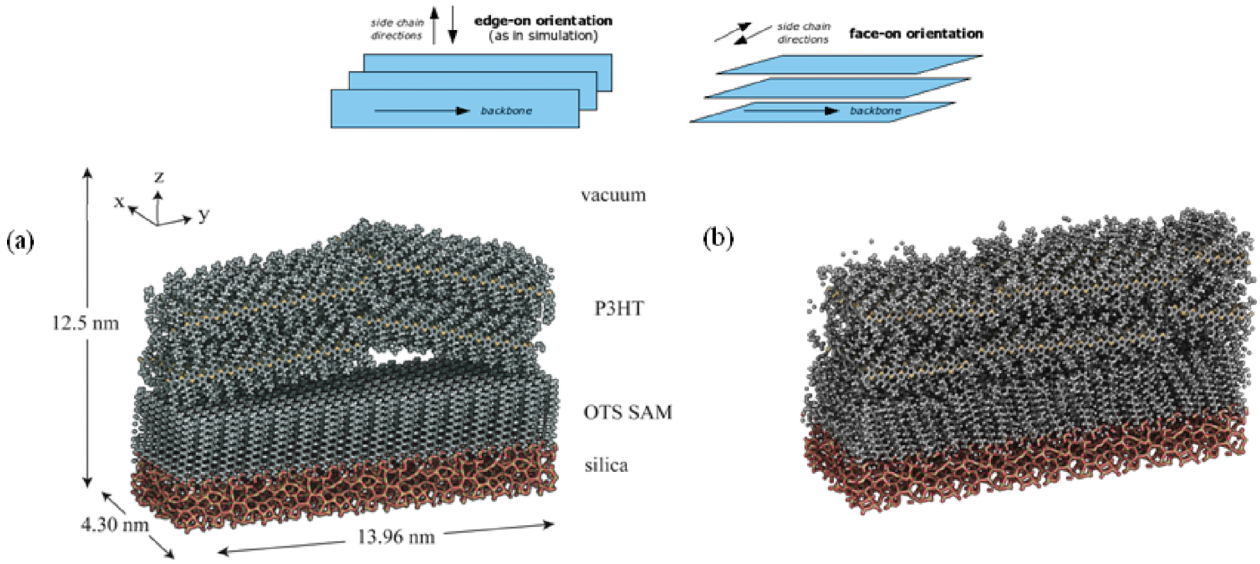

Figure 1. (a) Initial simulation geometry, prior to any simulation time. An edge-on P3HT crystal equilibrated in *isolation* under NPT conditions ($T = 300$ K) and consisting of 2 × 8 × 2 19-mers is placed in contact with an amorphous silica substrate and a SAM with a maximum of 240 OTS molecules. Visualization created with Qutemol.[36] (b) An example of an equilibrated simulation (order_66 from Table 1) after 2.999 ns of dynamics. Some P3HT backbones appear to be divided because they passed through a periodic boundary and appeared on the other side of the simulation cell.

and (3) $\langle S \rangle$ smaller than 0.5 (low orientational order). Perhaps counterintuitively, we find that disordered SAMs generate the highest $\langle S \rangle$ values. The ordered OTS monolayers, for the CH_3 and CF_3 end group chemistries considered here, produce the lowest degree of edge-on orientation in the P3HT crystallites (corresponding to an average ring tilt angle away from the vertical of ~45°), while disordered substrates correlate with increased P3HT orientational order (*i.e.*, larger values of $\langle S \rangle$ corresponding to an average ring tilt angle of ~23°). Several potential explanations for these results were ruled out; first, annealing and cooling simulations show that the ordering is not driven by the thermal motion of the OTS or the side chains. Second, the *trans*/*gauche* ratios of the P3HT side chains do not vary with changes in the order parameter. Instead, as we demonstrate in more detail below, the key difference between ordered and disordered substrates is that highly ordered SAMs present *disruptive energy minima* to P3HT molecules.

As illustrated in Figure 2, the gaps between perfectly packed OTS chains serve as potential energy wells for P3HT side chains, even though they are not large enough to permit interdigitation (which occurs only when the SAM is not fully dense). The energy displayed in Figure 2 represents the per-atom potential energy of the terminal C atoms on the P3HT side chains as they interact with the substrate; the reported energy is the sum of pair, bond, angle, dihedral, and improper terms. The extended deep potential energy wells and sharp energy peaks presented to the P3HT side chains by a well-ordered substrate can be seen in Figure 2. The perfectly packed OTS molecules are very restricted in their motion and remain close to their original lattice sites, shown in the figure as black dots. Low potential energy regions correspond to interstitial spaces between OTS close-packed directions, and high potential energies occur on or near OTS sites where side-chain terminal groups collide with the CH_3 groups on the OTS molecules. The three trajectories in the figure demonstrate that the P3HT side chains tend to linger in the energy wells and move abruptly away from regions of high potential energy. The wells on this ordered poten-

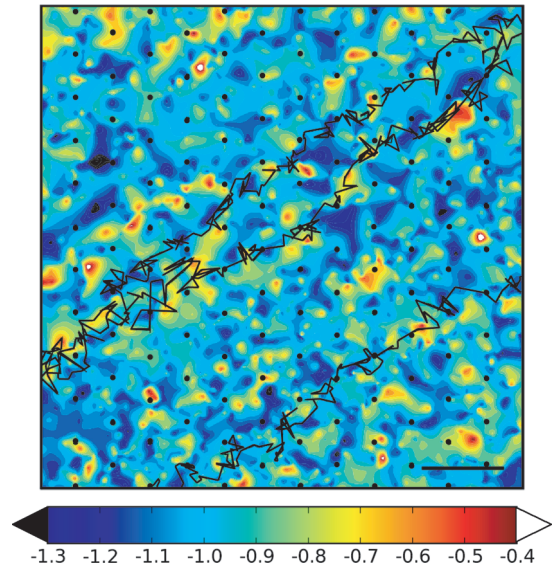

Figure 2. XY projection of typical per-atom potential energies (pair, bond, angle, dihedral, and improper contributions) of P3HT side-chain terminal C atoms that are nearest the OTS surface in the perfect_layer simulation. The three darker lines are trajectories for three individual C atoms. Black dots are the nominal positions of OTS molecules. These perfectly packed molecules create disruptive periodic energy minima for the P3HT side chains. Scale bar is 1 nm. Units of energy are kcal/mol.

tial energy surface strongly attract the P3HT side chains and encourage a face-on orientation in which the side chains lie flat on the substrate.

The predictions of the present work with regard to crystalline OTS monolayers may now be experimentally investigated. Recently, Ito *et al.*[30] demonstrated the ability to spin-coat essentially crystalline OTS monolayers on silica. Pentacene and fullerene thin films deposited on the crystalline OTS showed higher mobilities than films on more disordered OTS. These experimental results, however, do not contradict our predictions as pentacene and C_{60} lack the alkyl side chains that drive ordering in our simulations. No mobility measurements on polymeric thin films were reported.

The effects of partially disordered (*i.e.*, 33% and 67% disordered) SAMs were more complex; these simulations showed the greatest fluctuations in their order parameters over time. The fluctuations can be correlated with local variations in the surface potential, which in turn depended on how the OTS molecules had been randomly perturbed from perfect packing in the simulation setup. As a result of this randomization, some regions of the monolayer were highly ordered and others were disordered. In these simulations it was found that the P3HT chains moved continually around on the substrate attempting to find a stable configuration; however, such a configuration is unlikely due to the mixed ordered/disordered nature of these OTS

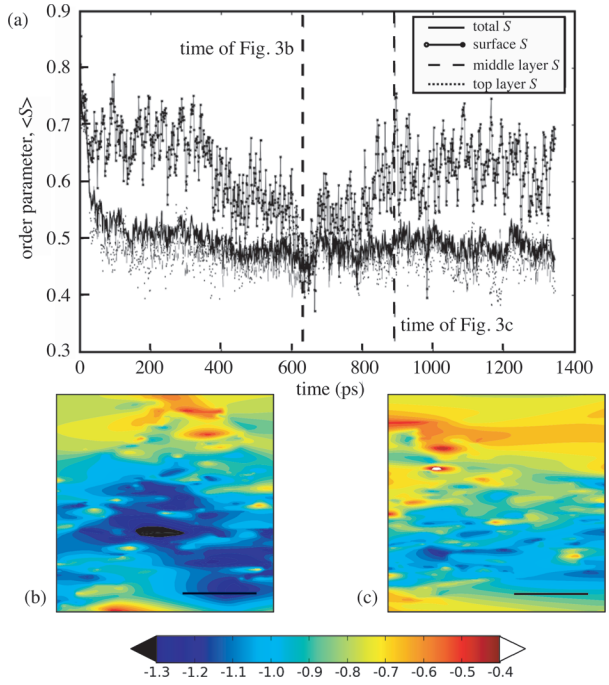

Figure 3. (a) Evolution in time of side-chain order parameters for the order_33 simulation. The total ⟨*S*⟩ is separated into contributions from side chains closest to the substrate, between the two layers of P3HT molecules, and at the top of the simulation box. (b) Surface potential energies of the terminal side-chain C atoms from 625 ps to 641 ps in Figure 3a, where ⟨*S*⟩ is low. Same quantity as panel b plotted from 884 ps to 900 ps, when ⟨*S*⟩ is high (c). Scale bars are 1 nm. Units of energy are kcal/mol.

SAMs. Thus, the P3HT side chains "wander" on the substrate energy landscape, interacting with both ordered and disordered OTS for prolonged periods of time. The influence of these local variations in surface potential is shown in Figure 3. The data illustrate the dependence of ⟨*S*⟩ on the local order at the interface. Figure 3a suggests that the P3HT morphology is strongly dependent on local substrate surface potential. The value of the orientational order parameter ⟨*S*⟩ for all P3HT side chains decreases sharply at approximately 620 ps after the beginning of the simulation, dominated by the side chains located directly at the monolayer/P3HT interface. At 825 ps, the order parameter for surface side chains increases dramatically, and the rest of the P3HT crystal trends toward greater order as well. This surface-mediated disordering and ordering is especially noteworthy since the near-surface P3HT side chains constitute only a small fraction of the total number of side chains, and entered into the total ⟨*S*⟩ calculation accordingly. Figure 3 panels b and c examine side-chain potential energies at the aforementioned times of relatively low (620 ps) and high (825 ps) surface side-chain order, respectively. Similar to Figure 2, Figure 3b exhibits wide regions of extremely low potential energy and relatively steep gradients, which correlate with low P3HT orientational order. Figure 3c, in contrast, has generally higher potential energy, with no deep potential energy wells, and more gentle gradients, hinting at greater substrate disorder. It was found that the end groups of the SAM molecules in these more disordered parts of the substrate are more mobile, oscillating far from their initial positions over time and presenting a relatively even surface of higher potential energy to the P3HT side chains. P3HT in contact with a surface of that nature displayed greater orientational order.

The cases in which P3HT was placed on a completely disordered SAM or on a bare amorphous SiO_2 surface gave the most stable edge-on orientation of the crystallites. Figure 4 shows near-surface P3HT side-chain potential energies on a bare SiO_2 substrate, which produced a high average order parameter ⟨*S*⟩. The surface potential, as experienced by P3HT side-chain terminal C atoms, is generally high, with only small energy wells. The energy wells are bounded by potential peaks, which screen their trapping effect on P3HT side chains. Thus, the bare SiO_2 surface does not show evidence of a high density of sites that can strongly attract the P3HT side chains and disrupt the P3HT orientation. Indeed, X-ray diffraction studies have shown that poly(thiophene) crystallites are well-oriented on bare SiO_2 surfaces.[22] Bare SiO_2 likely shows poor experimental device performance as a result of poorer longer-scale crystallinity of the polymer film and the presence of charge traps at the dielectric surface.[22] In light of these facts, we conclude that our findings in the bare_substrate trial are fully consistent with experi-

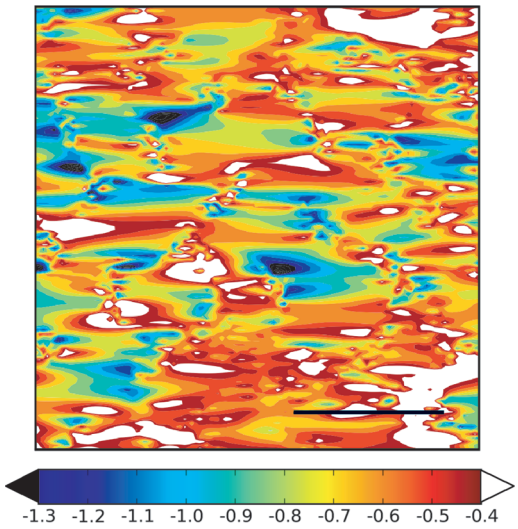

Figure 4. Surface potential energies of terminal side-chain C atoms in the bare substrate simulations. Scale bar is 1 nm. Units of energy are kcal/mol.

ment; we consider here only relatively short-range order and do not model charge transport or device properties.

We make a final note regarding P3HT backbone spacing in our simulations, which would relate to crystal d-spacing in a diffraction experiment. We calculated average nearest neighbor *minimum* backbone−backbone distances for all of our trials by examining the point of closest approach between monomers of neighboring backbones. We specifically excluded spacing in the *y*-direction in Figure 1, which corresponds to the ends of two P3HT backbones in contact, and focused on the more interesting case of packing in the *x* and *z* directions. We found that our minimum nearest neighbor distances varied by up to 5.1% depending on the degree of order $\langle S \rangle$. Trials with greater edge-on orientation tended to show larger P3HT backbone spacings. We attribute this to the fact that substrates that showed lower $\langle S \rangle$ order also had lower surface potentials and hence strongly attracted the P3HT side chains, pulling the molecules more tightly together. These variations in lattice spacings may have been undetected so far because in reported X-ray diffraction experiments, the OTS layer is solution-deposited and therefore inherently disordered. Thus, the orientational order parameter of the P3HT on the experimental OTS layer is similar to that on bare SiO_2. To the best of our knowledge, X-ray diffraction of P3HT on crystalline OTS layers has not been reported. Finally, X-ray diffraction probes the entirety of the film while our calculations only refer to the first two layers of polymer, which is where charge transport occurs.

CONCLUSIONS

This computational study indicates that the potential energy landscape created by the substrate for P3HT side chains affects the orientation of nanocrystallites of the polymer. From this main finding, we can make several predictions for further experimental and theoretical investigation. Perhaps surprisingly, perfectly ordered crystal-like substrates can disrupt ideal edge-on P3HT orientation if they present deep energy wells to the P3HT side chains. The disordered substrates considered here, which have energetically smoother and generally higher potential energy surfaces, encourage P3HT crystallite orientation closer to the ideal edge-on texture. High-energy substrates may be theoretically desirable as well since they would tend to minimize P3HT side-chain contact, thus favoring edge-on orientation; in practice, however, they are more susceptible to contamination. A chemically mixed monolayer, for example, might provide packing irregularities that would ultimately encourage edge-on P3HT alignment.

METHODS

The classical MD simulations described in this work employ the COMPASS forcefield[31] for all atom−atom interactions. The simulations were carried out using the LAMMPS (large-scale atomic/molecular massively parallel simulator) code[32] under constant particle number, volume, and temperature (*NVT*) conditions at a temperature of 300 K, using three-dimensional periodic boundary conditions. The equations of motion were integrated using the Verlet algorithm[33] with a time step of 1.0 fs. The nonbonded van der Waals interactions were treated by truncating atom pairs with an interatomic distance greater than $r_c = 15$ Å, coupled with a long-range tail correction.[34] The particle−particle particle−mesh Ewald (PPPM) method[35] was used for the long-range treatment of electrostatic interactions with a *k*-space accuracy set at 10^{-5}.

Acknowledgment. This work was performed under the auspices of the U.S. Department of Energy by Lawrence Livermore National Laboratory under Contract DE-AC52-07NA27344. A.S. acknowledges funding from the National Science Foundation, Career Award.

REFERENCES AND NOTES

1. Kim, D. H.; Park, Y. D.; Jang, Y.; Yang, H.; Kim, Y. H.; Han, J. I.; Moon, D. G.; Park, S.; Chang, T.; Chang, C.; Joo, M.; Ryu, C. Y.; Cho, K. Enhancement of Field-Effect Mobility Due to Surface-Mediated Molecular Ordering in Regioregular Polythiophene Thin Film Transistors. *Adv. Funct. Mater.* **2005**, *15*, 77–82.
2. Chang, J. F.; Sun, B.; Breiby, D. W.; Nielsen, M. M.; Solling, T. I.; Giles, M.; McCulloch, I.; Sirringhaus, H. Enhanced Mobility of Poly(3-hexylthiophene) Transistors by Spin-Coating from High-Boiling-Point Solvents. *Chem. Mater.* **2004**, *16*, 4772–4776.
3. Kline, R. J.; McGehee, M. D.; Kadnikova, E. N.; Liu, J.; Frechet, J. M. J.; Toney, M. F. Dependence of Regioregular Poly(3-hexylthiophene) Film Morphology and Field-Effect Mobility on Molecular Weight. *Macromolecules* **2005**, *38*, 3312–3319.

4. Sirringhaus, H.; Brown, P. J.; Friend, R. H.; Nielsen, M. M.; Bechgaard, K.; Langeveld-Voss, B. M. W.; Spiering, A. J. H.; Janssen, R. A. J.; Meijer, E. W.; Herwig, P.; Leeuw, D. M. d. Two-Dimensional Charge Transport in Self-organzied, High-Mobility Conjugated Polymers. *Nature* **1999**, *401*, 685–688.
5. Sirringhaus, H.; Wilson, R. J.; Friend, R. H.; Inbasekaran, M.; Wu, W.; Woo, E. P.; Grell, M.; Bradley, D. D. C. Mobility Enhancement in Conjugated Polymer Field-Effect Transistors through Chain Alignment in a Liquid-Crystalline Phase. *Appl. Phys. Lett.* **2000**, *77*, 406–408.
6. Zen, A.; Pflaum, J.; Hirschmann, S.; Zhuang, W.; Jaiser, F.; Asawapirom, U.; Rabe, J. P.; Scherf, U.; Neher, D. Effect of Molecular Weight and Annealing of Poly(3-hexylthiophene)s on the Performance of Organic Field-Effect Transistors. *Adv. Funct. Mater.* **2004**, *14*, 757–764.
7. Chabinyc, M. L.; Lujan, R.; Endicott, F.; Toney, M. F.; McCulloch, I.; Heeney, M. Effects of the Surface Roughness of Plastic-Compatible Inorganic Dielectrics on Polymeric Thin Film Transistors. *Appl. Phys. Lett.* **2007**, *90*, 233508.
8. DeLongchamp, D. M.; Kline, R. J.; Lin, E. K.; Fischer, D. A.; Richter, L. J.; Lucas, L. A.; Heeney, M.; McCulloch, I.; Northrup, J. E. High Carrier Mobility Polythiophene Thin Films: Structure Determination by Experiment and Theory. *Adv. Mater.* **2007**, *19*, 833.
9. Salleo, A. Charge Transport in Polymeric Transistors. *Mater. Today* **2007**, *10*, 38–45.
10. Kline, R. J.; McGehee, M. D.; Kadnikova, E. N.; Liu, J.; Frèchet, J. M. J. Controlling the Field-Effect Mobility of Regioregular Polythiophene by Changing the Molecular Weight. *Adv. Mater.* **2003**, *15*, 1519–1522.
11. Salleo, A.; Jimison, L. H.; Donovan, M. M.; Chabinyc, M. L.; Toney, M. F. , Microstructural Effects on the Performance of Poly(thiophene) Field-Effect Transistors. In *Organic Field-Effect Transistors V*, 1st ed.; SPIE: San Diego, CA, 2006; Vol. 6336, p 63360C-8.
12. Chabinyc, M. L.; Jimison, L. H.; Rivnay, J.; Salleo, A. Connecting Electrical and Molecular Properties of Semiconducting Polymers for Thin-Film Transistors. *MRS Bull.* **2008**, *33*, 683–689.
13. Mayer, A. C.; Scully, S. R.; Hardin, B. E.; Rowell, M. W.; McGehee, M. D. Polymer-Based Solar Cells. *Mater. Today* **2007**, *10*, 28–33.
14. Chua, L.-L.; Zaumseil, J.; Chang, J.-F.; Ou, E. C. W.; Ho, P. K. H.; Sirringhaus, H.; Friend, R. H. General Observation of N-Type Field-Effect Behaviour in Organic Semiconductors. *Nature* **2005**, *434*, 194–199.
15. Kline, R. J.; McGehee, M. D.; Toney, M. F. Highly Oriented Crystals at the Buried Interface in Polythiophene Thin-Film Transistors. *Nat. Mater.* **2006**, *5*, 222–228.
16. Chabinyc, M. L.; Salleo, A.; Wu, Y. L.; Liu, P.; Ong, B. S.; Heeney, M.; McCulloch, I. Lamination Method for the Study of Interfaces in Polymeric Thin Film Transistors. *J. Am. Chem. Soc.* **2004**, *126*, 13928–13929.
17. Kim, D. H.; Jang, Y.; Park, Y. D.; Cho, K. Layered Molecular Ordering of Self-Organized Poly(3-hexylthiophene) Thin Films on Hydrophobized Surfaces. *Macromolecules* **2006**, *39*, 5843–5847.
18. Park, J.-H.; Kang, S.-J.; Park, J.-W.; Lim, B.; Kim, D.-Y. Enhancement of Field Effect Mobility of Poly(3-hexylthiophene) Thin Film Transistors by Soft-Lithographical Nanopatterning on the Gate-Dielectric Surface. *Appl. Phys. Lett.* **2007**, *91*, 222108.
19. Majewski, L. A.; Kingsley, J. W.; Balocco, C.; Song, A. M. Influence of Processing Conditions on the Stability of Poly(3-hexylthiophene)-Based Field-Effect Transistors. *Appl. Phys. Lett.* **2006**, *88*, 222108–3.
20. Ong, B. S.; Wu, Y.; Liu, P.; Gardner, S. Structurally Ordered Polythiophene Nanoparticles for High-Performance Organic Thin-Film Transistors. *Adv. Mater.* **2005**, *17*, 1141–1144.
21. Salleo, A.; Chabinyc, M.; Yang, M.; Street, R. Polymer Thin-Film Transistors with Chemically Modified Dielectric Interfaces. *Appl. Phys. Lett.* **2002**, *81*, 4383–4385.
22. Jimison, L. H.; Salleo, A.; Chabinyc, M. L.; Bernstein, D. P.; Toney, M. F. Correlating the Microstructure of Thin Films of Poly[5,5-bis(3-dodecyl-2-thienyl)-2,2-bithiophene] with Charge Transport: Effect of Dielectric Surface Energy and Thermal Annealing. *Phys. Rev. B* **2008**, *78*, 125319.
23. Jung, Y. S.; Kline, J.; Fischer, D. A.; Lin, E. K.; Heeney, M.; McCulloch, I.; DeLongchamp, D. M. The Effect of Interfacial Roughness on the Thin Film Morphology and Charge Transport of High-Performance Polythiophenes. *Adv. Funct. Mater.* **2008**, *18*, 742.
24. Komeda, T.; Namba, K.; Nishioka, Y., Octadecyltrichlorosilane Self-Assembled-Monolayer Islands as a Self-Patterned-Mask for HF Etching of SiO_2 on Si. *Papers from the 44th National Symposium of the AVS*, 3 ed.; American Vacuum Society: San Jose, CA, 1998; Vol. 16, pp 1680−1685.
25. Brzoska, J. B.; Azouz, I. B.; Rondelez, F. Silanization of Solid Substrates: A Step Toward Reproducibility. *Langmuir* **1994**, *10*, 4367–4373.
26. Kojio, K.; Ge, S.; Takahara, A.; Kajiyama, T. Molecular Aggregation State of *n*-Octadecyltrichlorosilane Monolayer Prepared at an Air/Water Interface. *Langmuir* **1998**, *14*, 971–974.
27. Parikh, A. N.; Allara, D. L.; Azouz, I. B.; Rondelez, F. An Intrinsic Relationship between Molecular Structure in Self-Assembled *n*-Alkylsiloxane Monolayers and Deposition Temperature. *J. Phys. Chem.* **1994**, *98*, 7577–7590.
28. Srinivasan, U.; Houston, M. R.; Howe, R. T.; Maboudian, R. Alkyltrichlorosilane-Based Self-Assembled Monolayer Films for Stiction Reduction in Silicon Micromachines. *J. MEMS* **1998**, *7*, 252–260.
29. Kim, D. H.; Jang, Y.; Park, Y. D.; Cho, K. Surface-Induced Conformational Changes in Poly(3-hexylthiophene) Monolayer Films. *Langmuir* **2005**, *21*, 3203–3206.
30. Ito, Y.; Virkar, A. A.; Mannsfeld, S.; Oh, J. H.; Toney, M.; Locklin, J.; Bao, Z. Crystalline Ultrasmooth Self-Assembled Monolayers of Alkylsilanes for Organic Field-Effect Transistors. *J. Am. Chem. Soc.* **2009**, *131*, 9396–9404.
31. Sun, H. COMPASS: An *ab Initio* Force-Field Optimized for Condensed-Phase Applications—Overview with Details on Alkane and Benzene Compounds. *J. Phys. Chem. B* **1998**, *102*, 7338–7364.
32. Plimpton, S. Fast Parallel Algorithms for Short-Range Molecular-Dynamics. *J. Comput. Phys.* **1995**, *117*, 1–19.
33. Verlet, L. Computer Experiments on Classical Fluids. I. Thermodynamical Properties of Lennard-Jones Molecules. *Phys. Rev.* **1967**, *159*, 98.
34. Allen, M.; Tildesley, D. *Computer Simulation of Liquids*; Oxford Press: Oxford, England, 1989.
35. Hockney, R.; Eastwood, J. *Computer Simulation Using Particles*; McGraw-Hill: New York, 1981.
36. Tarini, M.; Cignoni, P.; Montani, C. Ambient Occlusion and Edge Cueing for Enhancing Real Time Molecular Visualization. *IEEE Trans. Visualization Comput. Graphics* **2006**, *12*, 1237–1244.